Rider's Head Injury Risks in Relation to Dynamics of Motorcycle in Frontal Crashes

Z. M. Jawi[1,2], K. S. Tan[*1], M. S. Risby[1], C. P. Ng[1], W. P. Loh[3], K. A. Abu Kassim[2] and Y. Ahmad[2]

[1]Department of Mechanical Engineering, Faculty of Engineering, Universiti Pertahanan Nasional Malaysia, Kem Sungai Besi, 57000 Kuala Lumpur, Malaysia
[2]Malaysian Institute of Road Safety Research (MIROS), 43000 Kajang, Malaysia
[3]School of Mechanical Engineering, Universiti Sains Malaysia, 14300 Nibong Tebal, Pulau Pinang, Malaysia

*Corresponding author: keansheng@upnm.edu.my

ORIGINAL ARTICLE   **Open Access**

Abstract – *Motorcycle frontal crashes usually cause serious and fatal head injuries to riders. This paper presents a two-level factorial experiment through finite element simulations of motorcycle-rigid wall impact scenario to investigate the effects of motorcycle layout design variations on rider's relative head injury risks, and also of the deformation mechanisms of motorcycle frontal structures on dynamics of the motorcycle. The motorcycle layout design variations were represented by the changes of three design factors, namely location of the engine block, location of air filter casing and its orientation. Head Injury Criteria (HIC_{15}) based on a time interval of 15 ms were selected as the response variable to evaluate the effects of the corresponding changes. The analysis showed that HIC_{15} values were significantly influenced by the changes of these factors, with the differences ranging from -21% to +11% for seven different designs of motorcycle layout as compared to the original one. Such influences on HIC_{15} values were mainly due to the changes in motorcycle dynamics caused by different deformation mechanisms of the wheel, which was attributed to interactions between the frontal structures and the engine block and also air filter casing. It was also found that HIC_{15} values were significantly influenced by the vertical component of motorcycle accelerations, but not by the horizontal component. A regression model for predicting the HIC_{15} value was established and the effect plots of the factors were also produced from the factorial analysis and it was found that there were interactions between the effect of the design factors. The outcomes of the present study provide an insight into how the structural response of the frontal structures of motorcycles could be taken into consideration as part of design elements in reducing rider's head injury risks in frontal crashes.*

Keywords: Rider's head injury risks, Head Injury Criteria (HIC), motorcycle crash simulations, small motorcycle crash safety, motorcycle dynamics

1.0 INTRODUCTION

In the context of the ASEAN road safety scenario, in which motorcyclists represent over 90 per cent of the total number of road users in the region (ASEAN Statistics Division, 2020) and with tremendously high fatality rates, making cars to be more motorcyclist-friendly is especially crucial. As a continuous effort of ASEAN NCAP's strategic approaches in reducing the number of accidents and injuries involving motorcyclists in the region, Motorcyclists Safety will be included as one of the four main pillars of ASEAN NCAP protocol from 2021 onwards (Abu Kassim et al., 2018). The assessment elements will include Blind Spot Detection, Blind Spot Visualization, Advanced Rear View Mirror, Auto High Beam, Advanced Motorcyclist Safety Technology. These are the active countermeasures to prevent a crash. These features represent active safety measures in an effort to totally avoid crashes. However, on the other hand, it is undoubtedly that contacts and crashes are essentially unavoidable and it is where passive safety measures come into play (Sporner et al., 1990; Berg et al., 1998). Thus, the importance of passive safety design features must not be overlooked and shall also be considered as part of the assessments in near future to enhance the comprehensiveness of the ASEAN NCAP rating system.

Efforts of developing passive safety features have been mostly focused on the motorcycle-rider system itself, such as motorcycle fitted airbag (Bhosale, 2013; Aikyo et al., 2015), rider's airbag jacket (Capitani et al., 2010; Grassi et al., 2018; Serre et al., 2019), and the head and neck protective device (Gobbi et al., 2019). In developing these effective passive safety measures, a clear understanding of the behaviours of motorcycles and riders when they interact with the opposing vehicle during crashes is of the utmost importance. There was a great deal of work devoted to studying the kinematics of motorcycle and rider, and the distributions and mechanisms of the injuries in crashes (Chinn et al., 2001; Toma et al., 2010; Serre et al., 2012; Carmai et al., 2019). Most of such works were focused on frontal, or Type I collisions, in which a motorcycle crashed directly onto an opponent vehicle because it has been well known to be the severest type of road crash. Such collision type is not only highly represented in statistics (Whitaker, 1980; Otte et al., 1981; Harms, 1989; Pang et al., 2000; Piantini et al., 2016) but also always leads to serious or fatal head injuries (Ramet et al., 1981; Sporner et al., 1990; Pang et al., 1999; MacLeod et al., 2010; Piantini et al, 2016) as the rider is often ejected from the motorcycle and thrown directly towards the opponent vehicle, with the head directly impacts with stiff parts of the vehicle.

While there was numerous research conducted to study the influences of vehicle front-end design on injury outcomes of pedestrians (Simms et al., 2006; Han et al., 2012; Li et al., 2017) and bicyclists (Maki & Kajzer, 2001; Fanta et al., 2013; Bourdet et al., 2014), not much of such research has been made for motorcycle impact scenario. Schaper and Grandel (1985) analysed dummy's kinematics in regard to interaction with motorcycle fuel tank and handlebar, and head impact on the car body in motorcycle-passenger car impact tests. It was reported that high head impact load was observed when structural car body parts were hit. Xiao et al. (2020) presented a comprehensive study in investigating the influences of impact scenarios and vehicle front-end design parameters on the head injury risk of the motorcyclist. The front-end design which is represented by bonnet design variations such as its length, height, angle and also windshield angle, were found to highly influenced motorcyclist's head injury risks during motorcycle-vehicle impacts. It was reported that, for instance, decreasing the bonnet angle and increasing the bonnet length can potentially reduce head injury risks. Nevertheless, there is also

a lack of work that looks in detail at how rider's head injury risks are associated with the dynamics of motorcycles in frontal crashes.

In this study, it was hypothesized that deformation mechanisms of the motorcycle frontal structures will significantly affect the dynamics of the motorcycle which then, in turn, affects the rider's injury risks. It is believed that sufficient knowledge gained in this subject matter will provide useful input for vehicle design consideration in improving design features of cars with respect to motorcyclist's safety. In view of this, the present study was carried out with the first objective to explore the feasibility of reducing the rider's head injury risks in frontal crashes by performing some modifications on the motorcycle layout design. It is then followed by the second objective to investigate the effects of dynamics of a motorcycle on rider's head injury risks, and the causes leading to such effects. The effects of layout design changes on the value of rider's Head Injury Criteria (HIC_{15}) based on the time interval of 15 ms in frontal crashes was investigated. The development of the complete model including the validations and the associated test methods are first presented, followed by the parametric study of the designs of the motorcycle using factorial experiment approach.

2.0 MODELLING AND SIMULATION

2.1 Setup of the Simulation Model

The present study used finite element simulation as the research tool to realize the modifications of the motorcycle layout. The motorcycle model used is based on one of the Malaysian national motorcycles, i.e. an early version of MODENAS Kriss 110. This motorcycle represents the most common type of motorcycle that is being used as daily transport in ASEAN countries. This type of motorcycle is typically characterized by an engine capacity of 125 ± 25 cc, mass of 100 ± 10 kg and wheelbase of 1250 ± 50 mm. In Malaysia, some of the popular models are Modenas GT128, Honda EX5, Yamaha 135LC, Suzuki Smash, etc.

In real-world crashes, particularly frontal crashes, the wheel and the fork assemblies are often experienced severe deformations (Pang, 2000). It was also observed that these frontal structures had already deformed severely even before the dummy began to experience significant forward sliding (Ariffin et al., 2016; Hamzah et al., 2014). Besides, it was indicated that the dynamics of the motorcycle and the dummy rider in frontal crashes were depended on the initial collapsing characteristics of the front wheel (Yettram et al., 1994), which could in turn influence the initial pitching dynamics and consequently affects behaviours of the rider. Thus, in order to capture more accurately the dynamics of motorcycles, these structures have to be modelled in detail. The level of modelling details was based on observations from crash tests (Ariffin et al., 2016; Hamzah et al., 2014) and also the component test outcomes (Tan et al., 2006; Tan et al., 2008). The wheel model incorporated an air-inflated tyre and wire-spoked wheel assembly, while the fork assembly was modelled with suspension capability, as illustrated in Figure 1. The detailed modelling and validation aspects of these two critical frontal structures are respectively available in (Tan et al., 2013) and (Tan et al., 2016).

The motorcycle model used had been validated by evaluating the kinematics of the motorcycle against physical test data of frontal impact with a moving rigid barrier using Roadside Safety Verification and Validation Program (RSVVP) (Mongiardini & Ray, 2009). Comparisons of the time histories are shown in Figure 2 whilst the evaluation metrics and also the evaluation outcomes are summarized in Table 1.

Table 1: Motorcycle validation outcomes using RSVVP

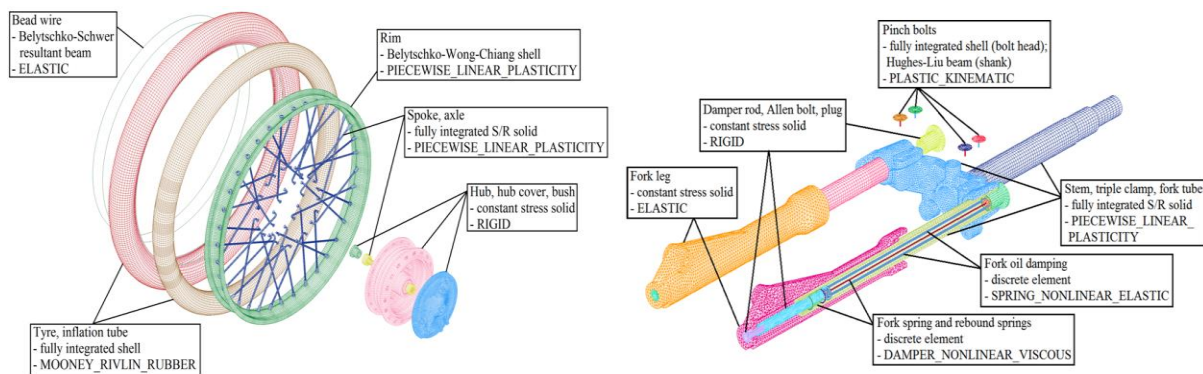| Response	Sprague-Geers MPC			ANOVA	
	Magnitude (40%)	Phase (40%)	Comprehensive (40%)	Average (5%)	Standard Deviation (35%)
x-acceleration	17.6	16.5	24.2	0.9	21.6
z-acceleration	-11	22.7	25.2	0.8	19.8
x-velocity	-3.5	19.7	20	4.3	24.2
z-velocity	1.9	7.5	7.7	4.4	14.9

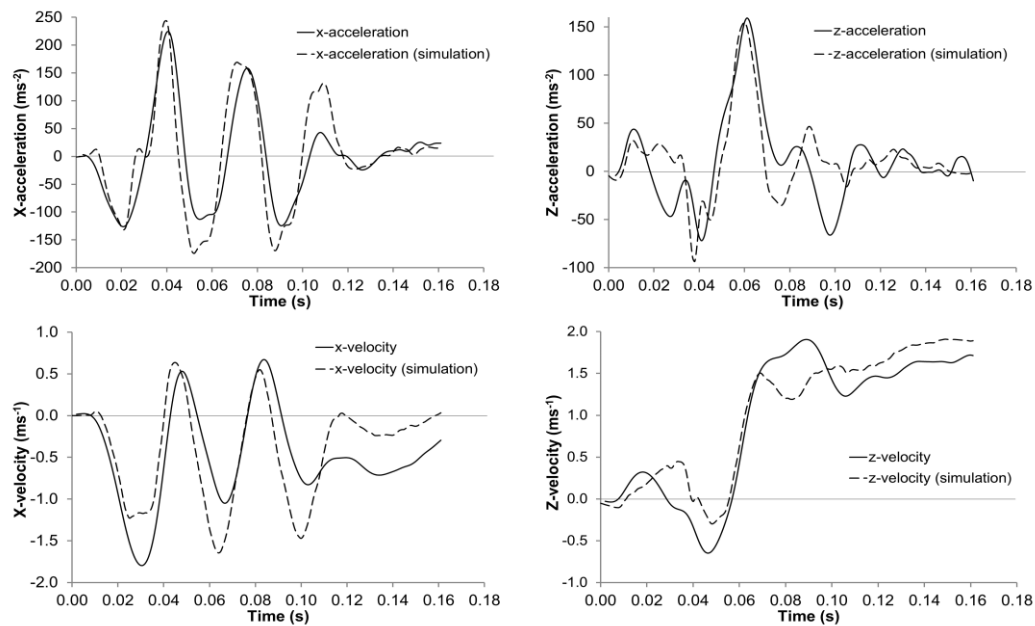**Figure 1:** Details of the models of wheel and fork assemblies

Figure 2: Comparisons of acceleration and velocity profiles between the simulation and the physical test

The Sprague-Geers MPC metrics measure the similarity between the test and simulation data curve shapes, while the ANOVA metrics evaluate the residual errors (Ray et al., 2012). The acceptance limit of the metrics, as indicated in the brackets for the respective metrics, were derived from the outcomes of typical normal variations that occurred in vehicle full-scale crash tests. It can be seen that the evaluated value of each metric was significantly lower than the acceptance limit, suggesting that the model was satisfactorily validated.

For the rider, since this is feasibility and exploratory type of study and the main focus is the head impact, thus the rider was represented by a simpler version of LSTC Hybrid III 5th Fast Dummy (Guha et al., 2011). Also, no helmet was fitted because the main analysis will be on the relative head injury risks among different motorcycle layouts. The dummy was positioned accordingly as on the motorcycle, with the palms resting on the handlebar and the shoes on the respective footrest. Besides, the rigid wall was used instead of deformable vehicle structure in order to exclude any effect from the opposing impacted structure so that the isolated deformation mechanism of the motorcycle frontal structures alone can be studied first.

2.2 Design of Experiment

The factorial design approach was used for the purpose of the parametric study to design the combination of factors. The identified factors of interest are the engine location (L_E), the air filter casing location (L_C) and its orientation (θ_C), as depicted in Figure 3.

Factor	Notation	Factor level	
		Low (-)	High (+)
Engine location (m)	L_E	0.357	0.397
Air filter casing location (m)	L_C	0.391	0.437
Air filter casing orientation (radian)	θ_C	1.117	1.571

Figure 3: Definition of the design factors

The L_E and L_C are measured from the axle while θ_C from the horizontal axis. By considering the layout of the actual motorcycle, the feasibility of adjusting the levels of these factors was very limited due to the confined space in the vicinity of the engine block and air filter casing. Thus, only two levels for each factor were considered in the current study. The original configuration of the engine and the casing were set as the low levels for the corresponding factors. With two-level 2^3 factorial design, there were eight different factorial treatments. The visualization of each of the combinations of the factors is illustrated in Figure 4.

The plus and negative signs denote respectively the high and low levels of the corresponding factors. The motorcycle model was to be altered accordingly and then used to simulation the frontal crash onto a rigid wall at an impact velocity of 11.11 ms^{-1} (40 km/h). The selected response variable was HIC$_{15}$.
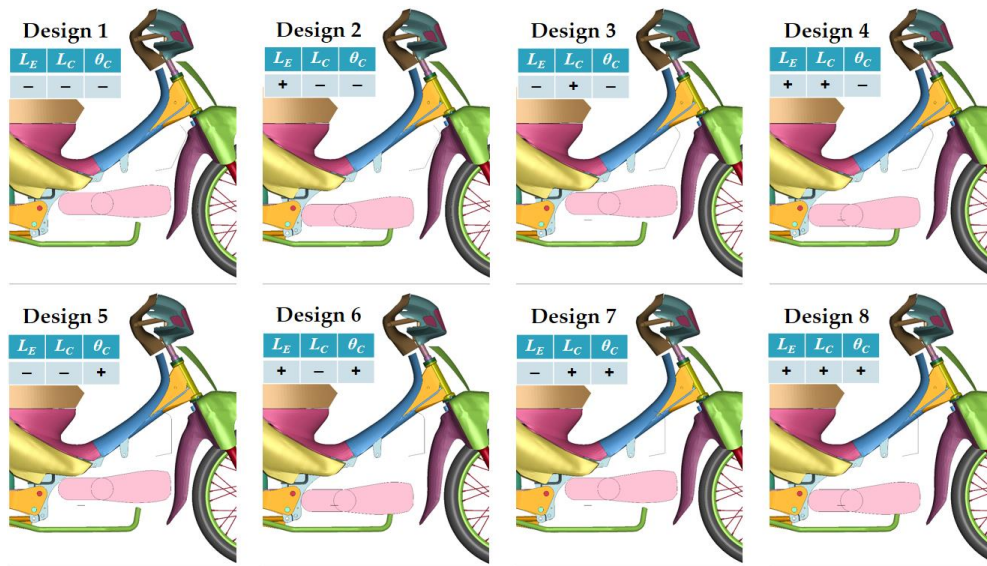
Figure 4: Visualization of the motorcycle layout with different combinations of the factors

3.0 RESULTS AND DISCUSSION

3.1 Overall Behaviours

The overall behaviour of the motorcycle and the rider of Design 1 in the crash simulation is depicted in Figure 5, from the first contact between the tire and the rigid wall until the head impacts the wall. Only Design 1 is presented here as an example for a discussion since the overall behaviour of other configurations are more or less the same by qualitative observation. The instant where the front tire just contacted the wall is regarded as time zero ($t = 0$).
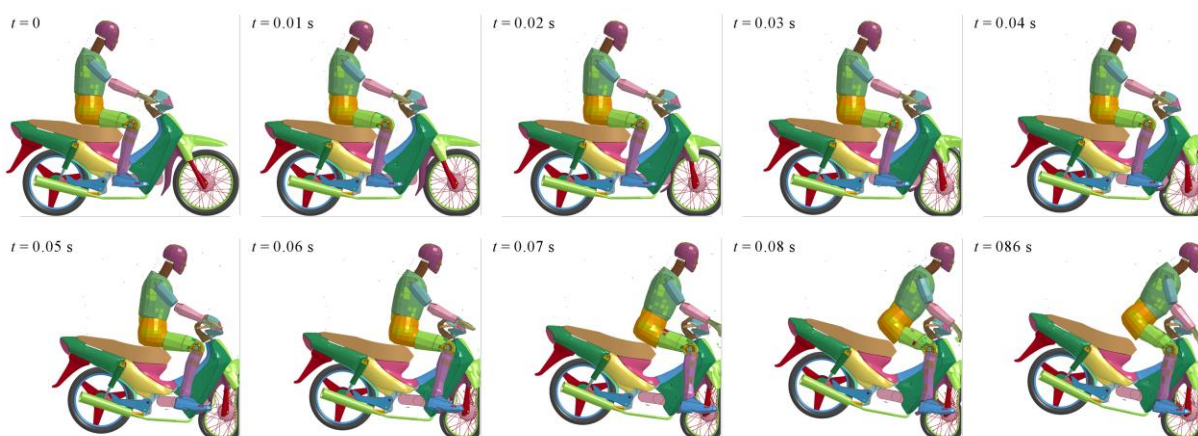

Figure 5: Overall behaviour of the simulated motorcycle-dummy system

The time histories of the velocity and acceleration components of the motorcycle and the dummy are presented in Figure 6. Upon the initial impact of the wheel on the wall, the tire immediately gets compressed, followed by the deformation of the rim at its frontal side, and then the deformations of the fork assembly through the fork tube bending and opening at the stem-triple clamp joint. Due to the quick response of the suspension mechanism, the fork

retracted and the motorcycle dived slightly as soon as the impact occurs. The diving was then recovered by some upward displacement of the frontal portion as the wheel deforming into an oval shape. The motorcycle only started to experience significant x-deceleration as the fork tube began to bend. The deceleration increased rather uniform and reached the peak at 0.02 s. The rider started to move forward relative to the motorcycle immediately after the impact since the rider was loosely sitting on the seat. However, the sliding motion of the rider was only becoming obvious from 0.02 s onwards after the first contact. Compared to the high-speed film of the full motorcycle crash tests (Ariffin et al., 2016; Hamzah et al., 2014), it was also found that the sliding becoming apparent at about the same time the maximum decelerations occurred.
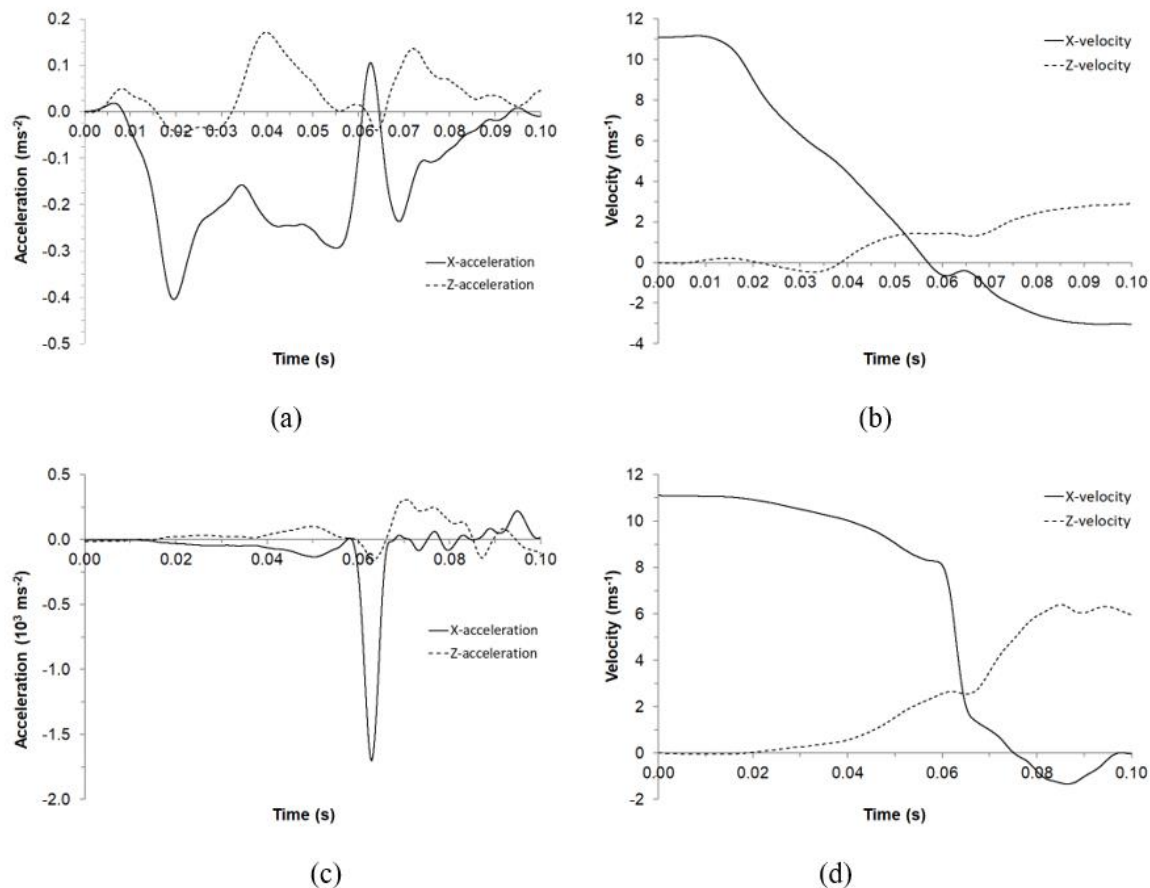

Figure 6: The time histories of (a) x- and z-accelerations, and (b) x- and z-velocities of the motorcycle; (c) x- and z-accelerations, and (d) x- and z-velocities of the dummy with reference to the H-point

Towards the end of this peak deceleration, the rear side of the rim started to deform under the compression by the engine block and the overall wheel deformed progressively into an oval shape. Such deforming process in turn progressively increased the tension of the spokes that are located at the upper region of the hub. The tensions eventually overcame the support of spoke nipples on the rim whereby the corresponding spokes suddenly get torn off from the rim. The final torn off occurred at 0.022 s, signified the end of the failure mechanism. Such failure caused the stiffness of the wheel to reduce significantly and so the resistance to the forward inertial load of the motorcycle is reduced. This is reflected by the dropping of the x-acceleration curve that starts at about 0.02 s and lasted until 0.025 s, which then follows by a reduced rate of deceleration until 0.034 s. This dropping is due to the increasing resistance against the

motorcycle inertial load that resulted from the increasing contact load between the air filter casing and the wheel. It was also found that at this time period, there is neither significant deformation at the stem-triple clamp joint nor the bending of the fork tube. On the other hand, following the torn off of the spokes from the rim, the hub and the axle lost the support and the front portion of the motorcycle started to dive, as indicated by the negative z-velocity, at 0.02 s. This occurred at a rather uniform velocity, or constant deceleration, for the interval between 0.02 to 0.029 s. The diving behaviour caused the motorcycle to become tended to pitch, with the rear tire observed to be started leaving the ground at about 0.02 s. The pitching effect progressively overtook the diving after 0.033 s where the acceleration becoming opposite to the downward velocity. The absolute pitching occurred at 0.038 s but the corresponding acceleration only lasted for a short while before the motion turned into uniform deceleration due to the counteraction of the dummy's weight and also the gravitational force.

As the motorcycle continued to advance forward, the rim then came into contact with the hub at 0.034 s. The rim eventually gets fully pressed against the wall such that the concave portion of the rim was flattened at about 0.038 s and the axle generally reached its maximum forward displacement. The fork assembly was also started to deform again after the hub contacted the rim. With the increased resistance to the forward motion, it can be seen that in this interval the deceleration started to increase again, followed then by a constant deceleration for an interval until 0.048 s. After 0.048 s, the upward deformation of the top portion of the rim progressively reaching the limit as constrained by the triple clamp. which in the other way round prevented the shortening of the fork and caused the diving due to the shortening of the fork was also reduced as the motion was obstructed by the wheel. The reducing deformation capacity of the frontal structures resulted in the uniformly increasing deceleration, which reached the maximum value for the interval at 0.056 s. It was found that this instant was coincided with the maximum total deformation of the frontal structures, as reflected in the plot of dissipated energy in Figure 7 that also shows the maximum value at about 0.056 s.
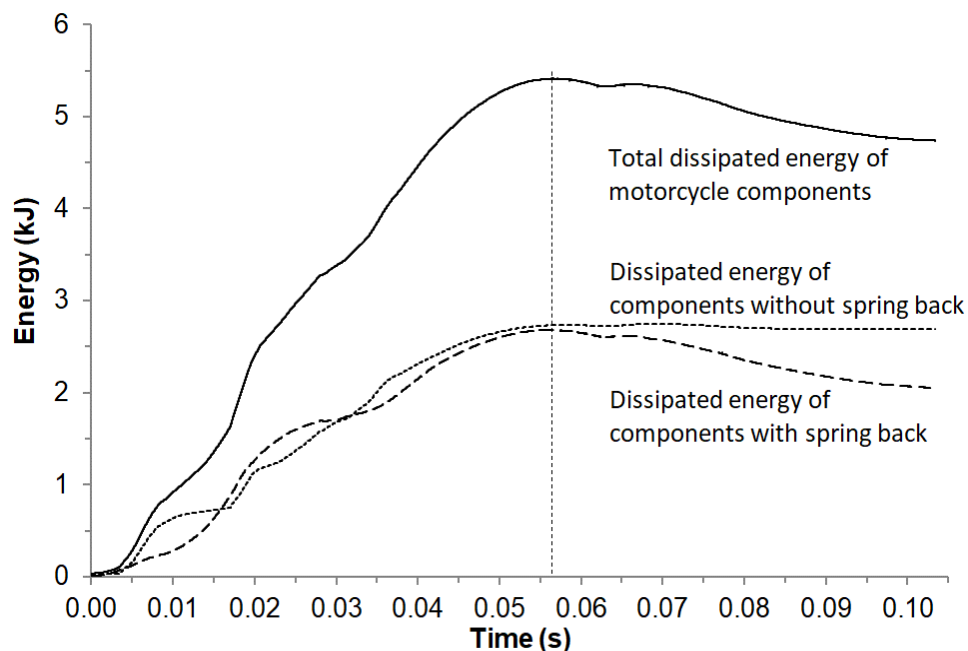

Figure 7: Energy dissipated by deformed components in the crash

At this instant, the impact event is regarded to reach the maximum engagement which is then followed by the separation phase. The negative x-velocity of the motorcycle from 0.056 s onwards indicates that it started to experience rearward movement, or rebound, with highly positive uniform acceleration that started from 0.056 s. Some parts, particularly steering stem, triple clamp and fork tubes, experienced spring back, along with recovery of the front suspension. This is shown by the significant drop in internal energy in Figure 7. For vertical motion, the inflated tire was observed to rebound at the end of the maximum engagement, in which the effect is reflected as the slight increase in the z-acceleration curve at the corresponding instant. In the subsequent motion, the horizontal rebound was interfered with by the occurrence of the knees hitting at both sides of the fenders at about 0.059 s, which obviously tended to push the motorcycle in an opposite direction.

Due to the counteraction, the rate of the increasing rebound velocity started to drop, which is also seen as a slight drop of the rate of positive uniform acceleration in the curve at the corresponding instant. The velocity then reached the turning point and started to reduce. However, the effect only lasted for a relatively short time and as it faded, the rebound velocity started to increase again. This can be seen by the dropping of the acceleration from its turning point at 0.063 s to zero at 0.065 s. On the other hand, the impact produced a clockwise moment about the axle which tended to cause pitching motion. However, as the motion was obstructed by the dummy's weight, the motorcycle experienced uniform deceleration right after the incident, as shown by the immediate drop in the z-acceleration at the corresponding instant, which lasted until 0.064 s. It was found that 0.064 s was indeed the time the buttocks start leaving the seat, which then allowed for the motorcycle pitching to continue, as signified by the uniformly increasing acceleration. The z-acceleration of the motorcycle eventually reached its maximum value as the effect of the disturbance faded and started to drop again and the rebound gained its acceleration again after 0.069 s. Towards the end of the incident, the knees slowly leaving the fender and the contact was fully disengaged at about 0.074 s. Both the x-acceleration and z-deceleration of the motorcycle then started to reduce uniformly until zero whereby the corresponding velocity components reached a constant value and will be finally dropped to zero.

The effect of the impact on the rider can be seen from the rapid increase of the deceleration of the H-point that also occurred from 0.059 s, then reached the peak value at 0.063 s, followed by rapid dropping until zero at 0.065 s. As mentioned above, the buttocks were started to leave the seat at 0.064 s, this indicated that only until this moment the rider was about to be fully ejected from the motorcycle, which in turn suggested that the dynamics of the motorcycle that occurred during the short interval before the pitching largely influenced the rider's subsequent behaviour. The deceleration is then followed by some fluctuations due to the contact by the seat. The main outcome of the incident was that the contact point formed a pivot that caused the rider to rotate clockwise, which eventually caused the forehead to hit on the rigid wall.

The sequential behaviours observed in the simulations are found to be generally consistent with the observations from motorcycle full-scale crash tests (Ariffin et al., 2016; Hamzah et al., 2014). However, in the current simulation, some key instances occurred slightly earlier as the target is rigid whereas it was a deformable structure of the car door in the physical test. All the time histories of the kinematics of the motorcycle and the rider in the simulations follow a similar trend, differs from each other mainly in terms of the magnitude and the incident time.

The filtered time histories of the rider's head acceleration corresponding to each of the motorcycle designs are presented in Figure 8. In general, two distinct groups of the curves demonstrate two major different head accelerations, of which the peak values occurred approximately at 0.0855 and 0.0868 s, respectively. The former corresponds to the design configurations of 1, 2, 3, 5, and 7, whereas the latter which is delayed by 0.001 s are of 4, 6, and 8. The peak values of the head acceleration a_{head}^{peak}, the HIC_{15} and the normalized HIC_{15} against HIC_{15} of each design are summarized in Table 2. The lowest peak acceleration occurred in design 1 whereas the highest in design 2 and 7. The same trend was also observed for the HIC_{15} values and the differences ranging from -21% to +11% for seven different designs of motorcycle layout as compared to the original one.
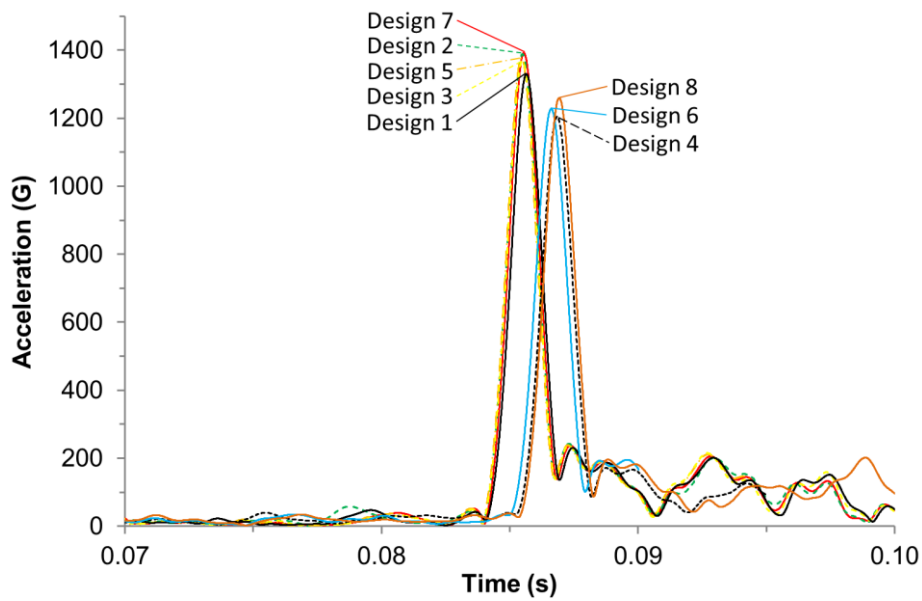

Figure 8: Rider's head accelerations in each configuration

Table 2: Responses of the motorcycle in terms of accelerations and energy absorbed in each of the treatments

		Factor Combination							
		1	**2**	**3**	**4**	**5**	**6**	**7**	**8**
Factor	L_E	–	+	–	+	–	+	–	+
	L_C	–	–	+	+	–	–	+	+
	θ_C	–	–	–	–	+	+	+	+
Response	a_{head}^{peak} (G)	1.33×10³	1.39×10³	1.37×10³	1.20×10³	1.38×10³	1.23×10³	1.39×10³	1.26×10³
	HIC_{15} (G)	5.21×10⁴	5.77×10⁴	5.57×10⁴	4.13×10⁴	5.63×10⁴	4.35×10⁴	5.75×10⁴	4.59×10⁴
	$(HIC_{15})_n$	1.00	1.11	1.07	0.79	1.08	0.84	1.10	0.88

Accelerations experienced by the motorcycle during the crash for each of the designs are presented in Figure 9. It is worth noting that in general, as has been identified in the response of head acceleration in Figure 8, two similar distinctive groups corresponding to the lower and higher HIC_{15} can also be identified respectively from the peak x-decelerations, and the z-accelerations. As indicated in Figure 9, for designs 3, 5, and 7, the peak x-decelerations are found to be totally not affected by the changes of the factor levels, with design 2 slightly higher compared to them, i.e. 8.7%. For another group, designs 4 and 8 have almost no difference in x-deceleration and are 4.9% lower than design 6. The difference between the minimum and maximum magnitudes is 35.1%, corresponds to the motorcycle design 7 and 6, respectively. While there are two apparent groups, no correlation was found between the x-acceleration and the HIC_{15}.
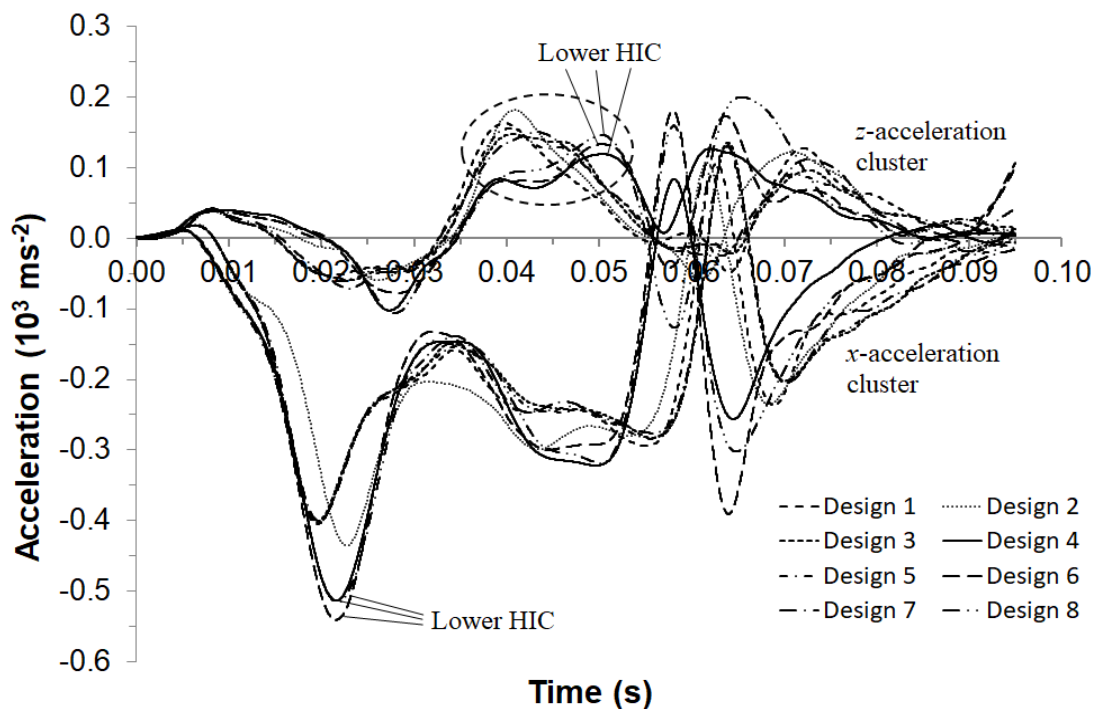

Figure 9: Accelerations of the motorcycle for all different designs

On the other hand, for z-acceleration, the two distinctive groups mainly differ in terms of the increasing rate of the acceleration that occurred within the short interval before reaching the maximum engagement, as highlighted in a circle of Figure 9. The peak magnitude of z-acceleration dropped significantly for as much as 34.4% from the highest value in design 2 to the lowest in design 4. The individual peak turning points corresponded to the moment the seat exerting force onto the buttocks. It is obvious that the HIC_{15} values increase with the rate of acceleration within this particular interval. In comparison to designs 1 and 2, design 4 exhibits a lower and smoother increasing rate and also the lower magnitude of z-acceleration for some duration during the pitching. On the other hand, wheel deformation mechanisms in design 2 were significantly different from design 4, whereby the rear side of the rim of design 2 undergone the severest localized bending. It was such localized deformation that facilitated the pitch motion as the engine block tended to stuck above the bent portion and produce additional moments about the axle.

3.2 Factorial Analysis

The factorial analysis was performed with a confidence level of 95%. The resulted main effects of the factor L_E, L_C and θ_C and the two-level interactions are presented in Figure 10.
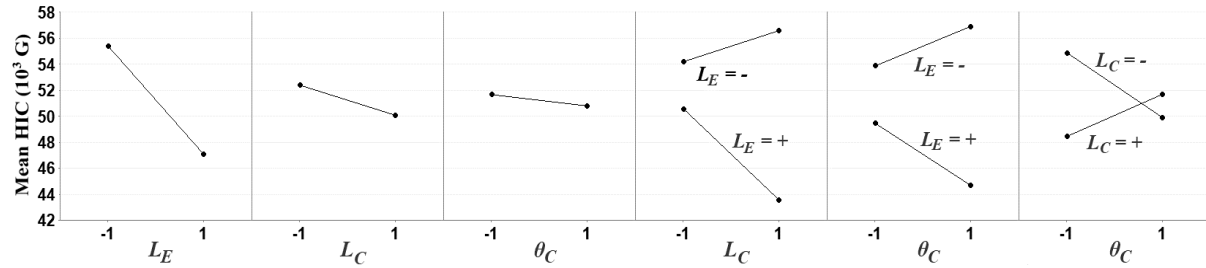

Figure 10: Main effect and interaction plots for the HIC^{15} as a response variable

The main effects plots, the three figures on the left, all show negative effects on the HIC_{15}. If it was considered only these three main effects, the motorcycle shall be designed with these factors at a high level as much as possible to minimize the HIC_{15}. However, another three figures on the right indicate that the interaction between any two of these factors are comparatively significant and the effects due to the interactions must be taken into design consideration. From the curves of L_E-L_C interaction plots, it can be clearly seen that the effect of casing location is greater when the engine location is at the low level ($L_E = -$) than at the high level ($L_E = +$). Also, the effects are opposite to each other i.e. increasing the casing location with the engine located at the high level tended to lower the HIC_{15} whereas the effect is contrary for engine location at the low level. When comparing the L_E-θ_C interaction plot, it shows that the L_E has the same trend when interacting with casing orientation, varying at about the same magnitude. The opposite trend occurs for L_C-θ_C interaction in which the curves intersect each other, whereby HIC_{15} increases with the casing orientation when L_C is at the high level but decreases when L_C is at the low level. For better visualization of these effects on the HIC_{15}, the empirical model yielded from the factorial analysis can be used to generate some curves as presented in Figure 11. The model is given as:

$$HIC_{15} = 10^5(- 6.423 + 24.815L_E + 13.447L_C - 0.025\theta_C - 51.005L_EL_C - 4.298L_E\theta_C + 3.929L_C\theta_C) \qquad (1)$$

Each of the graphs shown in Figure 11 demonstrates how HIC_{15} varies with the interacting factors. In each graph, there are two groups of curves respectively represented by solid and dashed lines, which show how HIC_{15} varies with the factors denoted by the legends in the graph. In each graph, there also exists a transition point correspond to a certain value of factor on abscissa where the other factor has inverse effect HIC_{15}. For example, in Figure 11 (c), the transition point occurs at about $\theta_C = 1.22$. For values lower and higher than this, L_C will affect HIC_{15} conversely.
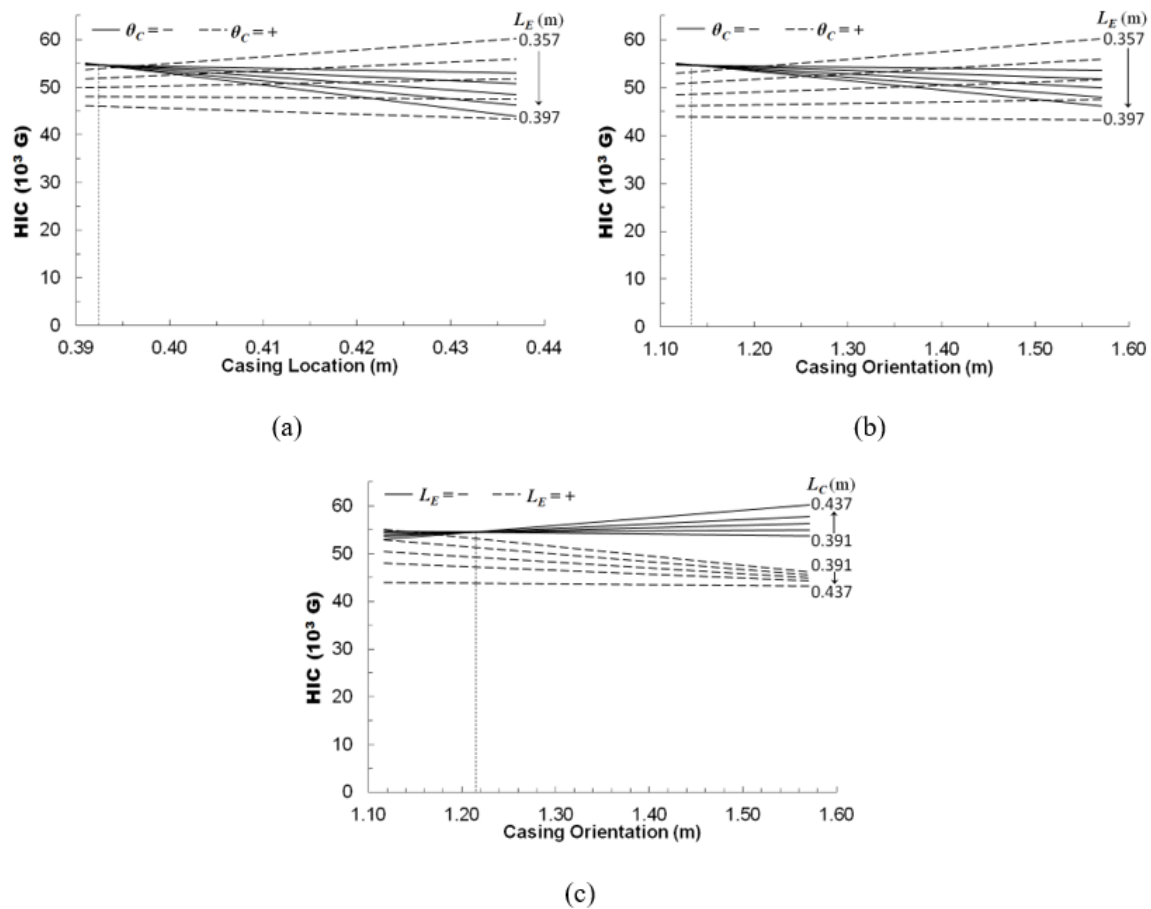
Figure 11: Plot of HIC$_{15}$ values against the corresponding factors shown for interactions of: (a) L_E-L_C; (b) L_E-θ_C; (c) L_C-θ_C

4.0 CONCLUSION

In the present study, a 2^3 factorial experiment using finite element simulations of motorcycle-rigid wall impact has been performed to investigate the effects of motorcycle layout design variations on rider's relative head injury risks, and also of the deformation mechanisms of motorcycle frontal structures on dynamics of the motorcycle. HIC$_{15}$ values were found to be significantly influenced by the changes of location of the engine block, location of air filter casing and its orientation. The differences for seven different designs of motorcycle layout ranged from -21% to +11% as compared to the original design. Such influences on HIC$_{15}$ values were mainly due to the changes in motorcycle dynamics caused by different deformation mechanisms of the wheel, which was attributed to interactions between the frontal structures and the engine block and also air filter casing. It is worth noting that the head accelerations and HIC$_{15}$ values were found to be significantly affected by the vertical component of motorcycle accelerations, but not by the horizontal component. There was no general trend of the changes of HIC$_{15}$ values based solely on any of the design factors, due to the existence of interactions of effects between the factors. The interaction caused the effect of a particular factor on the HIC$_{15}$ value to become significantly different as the other factor being varied from the value in the original design to the value at a high level. Thus, when performing modifications on motorcycle layout design in order to effectively reduce head injury risks, all the three factors considered in the present study must be optimized.

The simulations demonstrated the crucial of incorporating fully functional and deformable frontal structures in the model for effective design evaluation of the motorcycle for potential safety improvement. The outcomes of the present study provide an insight into how the structural response of the frontal structures of motorcycles could be taken into consideration as part of design elements in reducing rider's head injury risks in frontal crashes. Further studies by simulating impacts of a motorcycle to an opposing vehicle are substantially needed to allow for more comprehensive investigations on behaviours of a motorcycle-rider system as it interacts with various deformable car structures.

ACKNOWLEDGEMENTS

REFERENCES

Abu Kassim, K. A., Ahmad, Y., Mustaffa, S., & Mansor, M. R. A. (Eds.) (2018). ASEAN NCAP Roadmap 2021-2015. Selangor: New Car Assessment Program for Southeast Asian Countries.

Aikyo, Y., Kobayashi, Y., Akashi T., & Ishiwatari M. (2015). Feasibility study of airbag concept applicable to motorcycles without sufficient reaction structure. Traffic Injury Prevention, 16(sup1), S148-S152.

Ariffin, A. H., Solah, M. S., Hamzah, A., Isa, M. H. M., Jawi, Z. M., Yusoff, N. I. M. & Hainin, M. R. (2016). Exploratory study on airbag suitability for low engine capacity motorcycles. Jurnal Teknologi, 78(4), 65-69.

ASEAN Statistics Division. (2020). Total number of registered motorcycles (in thousand). Retrieved from https://data.aseanstats.org/indicator/ASE.TRP.ROD.B.011

Berg, F. A., Bürkle, H., Schmidts, F., & Epple, J. (1998). Analysis of the passive safety of motorcycles using accident investigations and crash tests. Proceedings of the 16th Technical Conference on the Enhanced Safety of Vehicles, 2221-2236.

Bhosale, P. V. (2013). Exploratory study on the suitability of an airbag for an Indian motorcycle using finite element computer simulations of rigid wall barrier tests. Proceedings of the 23rd International Technical Conference on the Enhanced Safety of Vehicles, Paper no. 13-0195.

Bourdet, N., Luttenberger, P., Teibinger, A., Mayer, C., Winllinger, R. (2014). Pedestrian and bicyclists head impact conditions against small electric vehicle. 2014 IRCOBI Conference Proceedings, 685-696.

Capitani, R., Pellari, S. S., & Lavezzi, R. (2010). Design and numerical evaluation of an airbag-jacket for motorcyclists. 4th International Conference Expert Symposium in Accident Research, Sept 16-18, Hannover, Germany, pp 147-158.

Carmai, J., Koetniyom, S., & Kassim, K. A. A. (2018). Analysis of rider and child pillion passenger kinematics along with injury mechanisms during motorcycle crash. Traffic Injury Prevention, 20(S1), S13-S20.

Chinn, B. P., Canaple, B., Derler, S., Doyle, D., Otte, D., Schuller, E., & Willinger, R. (2001). COST 327 Motorcycle Safety Helmets. Final report of the action. Retrieved from

https://ec.europa.eu/transport/road_safety/sites/roadsafety/files/pdf/projects_sources/cost327_final_report.pdf

Fanta, O., Bouček, J., Hadraba, D., & Jelen K. (2013). Influence of the front part of the vehicle and cyclist's sitting position on the severity of head injury in side collision. Acta of Bioengineering and Biomechanics, 15(1), 105-112.

Gobbi, M., Mastinu, G., & Previati, G. (2019). Motorcycle accidents – a new head and neck safety device for riders. International Journal of Automotive Technology, 20(1), 25-36.

Grassi, A., Barbani, D., Baldanzini, N., Barbieri, R., & Pierini, M. (2018). Belted safety jacket: A new concept in powered two-wheeler passive safety. Procedia Structural Integrity, 8, 573-593.

Guha, S., Bhalsod, D., & Krebs, J. (2011). LSTC Hybrid III 5th fast dummy positioning & post-processing documentation. MI: Livermore Software Technology Corporation.

Hamzah, A., Rahman, M. K., Ariffin, A. H., Solah, M. S., Paiman, N. F., Isa, M. H. M., Jawi, Z. M., & Kassim, K. A. A. (2014). Motorcycle structural response in simulated vehicular collision. Proceedings of International Crashworthiness Conference, Aug 25-28, Sarawak, Malaysia.

Han, Y., Yang, J., Nishimoto, K., Mizuno, K., Matsui, Y., Nakane, D., Wanami, S., & Hitosugi, M. (2012). Finite element analysis of kinematic behaviour and injuries to pedestrians in vehicle collisions. International Journal of Crashworthiness, 17(2), 141–152.

Harms, P. L. (1989). Leg injuries and mechanisms in motorcycle accidents. Proceedings of 12th International Conference on Experimental Safety Vehicles, Gothenburg, May.

Li, G., Lyons, M., Wang, B., Yang, J., Otte, D., & Simms, C. (2017). The influence of passenger car front shape on pedestrian injury risk observed from German in-depth accident data. Accident Analysis and Prevention, 101(2), 11–21.

MacLeod, J. B. A., Digiacomo, J. C., & Tinkoff, G. (2010). An evidence-based review: helmet efficacy to reduce head injury and mortality in motorcycle crashes: EAST practice management guidelines. The Journal of Trauma, Injury, Infection and Critical Care, 69(5), 1101–1111.

Maki, T., & Kajzer, J. (2001). The behavior of bicyclists in frontal and rear crash accidents with cars. JSAE Review, 22, 357-363.

Mongiardini, M., & Ray, M. H. (2009). Roadside safety verification and validation program (RSVVP) user's manual rev 1.4. Worcester Polytechnic Institute, Massachusetts, USA.

Otte, D., Kalbe, P., & Surgen, E. G. (1981). Typical injuries to the soft body parts and fractures of the motorised 2-wheelers. 1981 IRCOBI Conference Proceedings, 148-165.

Pang, T. Y. (2000). Injury characteristics of motorcyclists involved in motorcycle crashes in Klang valley (Unpublished master's thesis), Universiti Putra Malaysia, Selangor.

Pang, T. Y., Radin Umar, R. S., Azhar, A. A., Megat Ahmad, M. M. H., Nasir, M. T. M., & Harwant, S. (2000). Accident characteristics of injured motorcyclists in Malaysia. Medical Journal of Malaysia, 55(1), 45-50.

Pang, T. Y., Radin Umar, R. S., Azhar, A. A., Harwant, S., Wahid, S. A., Mansor, A. H., Noor, Z., & Othman, M. S. (1999). Fatal injuries in Malaysian motorcyclists. International Medical Research Journal, 3(2), 115-119.

Piantini, S., Pierini, M., Delogu, M., Baldanzini, N., Franci, A., Mangini, M., & Peris, A. (2016). Injury analysis of powered two-wheeler versus other-vehicle urban accidents. 2016 IRCOBI Conference Proceedings, 840-853.

Ray, M. H., Mongiardini, M., & Plaxico, C. A. (2012). Quantitative methods for assessing similarity between computational results and full-scale crash tests. Paper No. 12-2437. 2012 Transportation Research Board 91st Annual Meeting, Washington D.C.

Schaper, D., & Grandel, J. (1985). Motorcycle collisions with passenger cars: analysis of impact mechanism, kinematics, and effectiveness of full face safety helmets. SAE Transactions, 94, Section 1, 544-551.

Serre, T., Masson, C., Llari, M., Canu, B., Py, M., & Perrin, C. (2019). Airbag jacket for motorcyclists: evaluation of real effectiveness. 2019 IRCOBI Conference Proceedings, 533-547.

Serre, T., Masson, C., Perrin, C., Martin, J-L., Moskal, A., & Llari, M. (2012). The motorcyclist impact against a light vehicle: Epidemiological, accidentological and biomechanic analysis. Accident Analysis and Prevention, 49, 223-228.

Simms, C. K., & Wood, D. P. (2006). Pedestrian risk from cars and sport utility vehicles – a comparative analytical study. Proc. IMechE 220 Part D: J. Automobile Engineering, 220(8), 1085-1100.

Sporner, A., Langwieder, K., and Polauke, J. (1990). Passive safety for motorcyclists – from the leg protector to the airbag. SAE International Congress and Exposition, Detroit.

Tan, C. L., Tan, K. S., Lim, Y. T. & Wong, S. V. (2008). Experimental analysis on static and impact response of motorcycle front fork. Proceedings of International Crashworthiness Conference, July 22-25, Kyoto, Japan.

Tan, K. S., Wong, S. V., Megat Ahmad, M. M. H., & Radin Umar, R. S. (2016). Computational simulation of frontal impact of motorcycle telescopic fork. International Journal of Crashworthiness, 21(2), 161-172.

Tan, K. S., Wong, S. V., Megat Ahmad, M. M. H., Radin Umar, R. S., & Gupta, N. K. (2013). Computational simulation of fully deformable motorcycle wire-spoke wheel. Proceedings of Indian National Science Academy, 79(4), 639-650.

Tan, K. S., Wong, S. V., Radin Umar, R. S., Hamouda, A. M. S. & Gupta, N. K. (2006). An experimental study of deformation behaviour of motorcycle front wheel tyre assembly under frontal impact loading. International Journal of Impact Engineering, 32(10), 1554-1572.

Toma, M., Njilie, F. E. A., Ghajari, M., & Galvanetto, U. (2010). Assessing motorcycle crash related head injuries using finite element simulations. International Journal of Simulation Modelling, 9(3), 143–151.

Whitaker, J. (1980). Survey of Motorcycle Accidents. TRRL Laboratory Report LR913, Transport and Road Research Laboratory, Crow Thorne, Berkshire, U.K.

Xiao, Z., Wang, L., Mo, F. H., Lv, X. J., & Yang, C. H. (2020). Influences of impact scenarios and vehicle front-end design on head injury risk of motorcyclist. Accident Analysis and Prevention, 145, 105697.

Yettram, A. L., Happian-Smith, J., Mo, L. S. M., Macaulay, M. A., & Chinn, B. P. (1994). Computer simulation of motorcycle crash tests. Proceedings of 14th Int. Technical Conf. on the Enhanced Safety of Vehicles, May 23-26, Munich, Germany, 1994.